THE ASTROPHYSICAL JOURNAL, 406:614–628, 1993 April 1

FRAGMENTATION OF ELONGATED CYLINDRICAL CLOUDS. VI. COMPARISON WITH OBSERVATIONS

IAN BONNELL[1] AND PIERRE BASTIEN
Montreal Star Formation Group, Département de Physique, Université de Montréal, C.P. 6128, Succ. A, Montréal, Québec, Canada H3C 3J7; and Observatoire du Mont-Mégantic
Received 1992 June 16; accepted 1992 September 28

ABSTRACT

A comparison of hydrodynamical simulations of the collapse and fragmentation of elongated clouds with observations of molecular cores, star formation regions, and binary and multiple systems is presented. Observations of molecular cloud cores suggest appropriate initial conditions for numerical simulations of star formation. They include an elongated structure with rotation about an arbitrary axis and low values of β, the ratio of the absolute value of rotational to gravitational energies. The environments of young stellar objects display "warped" disks, and "bridges" of matter between young binaries, both of which are formed in our simulations. The kinematics of star-forming regions are explored, and a model is proposed where large line widths are explained by the dynamical process of infall and star formation.

Simulations of the formation and continued accretion of non–equal-mass binary systems are compared with observed differential reddening and IR companions in pre–main-sequence (PMS) binaries. The presence of an infrared companion could also explain the flat spectral energy distribution of some PMS stars.

The properties of main-sequence binaries are discussed with a view to the numerical models. The formation of binary systems from the fragmentation of elongated clouds easily explains the large eccentricities observed and the period-eccentricity relation. A spread in eccentricities arises through dissipative disk-disk interactions at closest approach. All separations greater than 50 AU can be explained by the numerical simulations, while separations less than 50 AU are possible (but have not yet been attained) with lower initial β or greater disk-disk interactions.

The formation of multiple systems is also discussed, and the observation of noncoplanarity in at least 35% of the multiple systems is explained in terms of the fragmentation of an elongated cloud with rotation about an arbitrary axis. The difference in mass ratios between the inner and outer systems can also be explained in terms of the different fragmentation processes involved.

Subject headings: binaries: visual — hydrodynamics — stars: formation — stars: pre–main-sequence

1. INTRODUCTION

In this paper we present comparisons of the work presented in previous papers of this series, with observations of star-forming regions, pre–main-sequence (PMS) objects, and main-sequence binary and multiple stars. The fragmentation of elongated clouds has been studied in the context of line fragmentation in the isothermal (Bastien et al. 1991, hereafter Paper I) and the polytropic (Arcoragi et al. 1991, hereafter Paper II) regimes. In both papers the dependence on the initial Jeans number, J_0, the ratio of the absolute value of gravitational to thermal energies, of the final number of fragments was studied for different cloud elongations, defined as L/D. Initial perturbations were applied along the cloud's major axis. For low J_0, the maximum number of fragments depended on J_0, while at large J_0 it was independent of J_0 but depended on the initial cloud elongation. In the polytropic regime (Paper II), the slope of the number of fragments versus J_0 depended on the polytropic constant for low J_0, while the same saturation occurred for large J_0.

The fragmentation of elongated clouds was first studied by Larson (1972). He found that two subcondensations can form along the major axis on either side of the equatorial plane. Bastien (1983) and Rouleau & Bastien (1990) investigated the details of the fragmentation and ascertained that the two fragments were gravitationally bound. The two fragments thus formed could form a binary system, provided that they did not collide at the cloud's center. Bonnell et al. (1991, hereafter Paper III) incorporated rotation perpendicular to the major axis ("end over end") into the initial conditions, defined by $\beta_\perp$, the ratio of the absolute value of rotational to gravitational energy for rotation perpendicular to the major axis. The collapse formed two fragments with surrounding disks and sufficient orbital angular momentum to avoid colliding. The binary systems formed by this process have high initial eccentricities. When rotation about an arbitrary axis is included, the initially high eccentricity can be reduced by dissipative encounters at closest approach (Bonnell et al. 1992, hereafter Paper IV). Rotation about an arbitrary axis is parameterized by $\beta_\perp$ and $\beta_\parallel$, the ratio of the absolute value of rotational to gravitational energies for the component of rotation parallel to the major axis. Bonnell & Bastien (1993) investigate the fragmentation of centrally condensed elongated clouds and find that moderately centrally condensed initial conditions fragment easily but r^{-1} distributions require differential rotation to fragment. Bonnell & Bastien (1992a, hereafter Paper V) studied the effect of the initial conditions on the binary's mass ratio. They found that small initial density gradients along the major axis are sufficient to form binary systems with unequal mass ratios ($0.1 \leq q = m_2/m_1 \leq 1.0$).

Subfragmentation of the two binary fragments was first proposed by Bonnell & Bastien (1991) for the collapse of elongated

[1] Present address: Institute of Astronomy, Madingley Road, Cambridge, CB3 0HA, England.

clouds rotating parallel to their major axis. In this scenario, for J_0 relatively large, the two fragments form in the shape of toroids with density minima on the major axis. The fragmentation of such toroids has been investigated by Norman & Wilson (1978). They found that the toroid is unstable to nonaxisymmetric perturbations and thus fragments into two or three subcondensations. In Paper IV we repeated the above calculations, including rotation about an arbitrary axis, with a three-dimensional smoothed particle hydrodynamics (SPH) code and found that the transfer of angular momentum by gravitational torques was too efficient to allow the toroid to form. Instead, the two fragments formed with surrounding disks. The fragments themselves sometimes formed in the shape of a bar which fragmented into two subcondensations. Further, if the bar did not fragment, it would redistribute the angular momenta into the disk, which could then fragment due to tidal forces. Another method of forming a multiple system from the fragmentation of elongated clouds was found in Paper III. For sufficiently large J_0, $J_0 = 3$, the collapse of an elongated cylinder, with rotation only perpendicular to the major axis, can form a bridge of material between the two fragments with sufficient mass to form one or more additional fragments.

In § 2 we discuss the appropriate initial conditions for star formation. The young stellar object (YSO) environment is discussed in § 3. An analysis of the kinematics of star-forming regions is presented in § 4, and § 5 presents a comparison with several star-forming regions. PMS binaries are discussed in § 6, while main-sequence binaries are discussed in § 7. A comparison with observations of multiple stars is included in § 8. A summary and conclusions are presented in § 9.

2. MOLECULAR CORES: INITIAL CONDITIONS

Star formation occurs in dense, cold molecular cloud cores where most of the process is obscured. As the dynamic collapse phase is therefore not directly observable, we will concentrate on the periods before and after gravitational collapse.

The intial conditions of star formation can be constrained by observations of molecular clouds and cores in which no stars have as yet formed. Of primary importance is the cloud's initial geometry and dynamics. Observations of giant molecular clouds have provided a wealth of information on different star-forming regions. The clouds are full of structure on many different scales. The filamentary nature of these clouds is apparent on the optical pictures of dark clouds cataloged by Schneider & Elmegreen (1979). Observations at radio wavelengths have also shown the complex, often filamentary nature of giant molecular clouds such as Orion (Bally et al. 1987), Taurus (Ungerechts & Thaddeus 1987), and Ophiuchus (Loren 1989a). Many elongated cores can be observed in these clouds with the direction of elongation parallel to that of the cloud (Loren 1989a). The observed periodicity in the core distribution in Orion A (Dutrey et al. 1991) can be compared with the results of Papers I and II. The equal spacing between cores suggests that they were formed through the fragmentation of the long filament.

Observations of molecular cloud cores (e.g., Myers et al. 1991; Lada, Bally, & Stark 1991) have found the average degree of elongation to be about 2, while Loren (1989a) finds that clumps in Ophiuchus have ratios of major to minor axes between 6 and 9. The actual core elongation is greater when projection effects are considered. Myers et al. (1991a) have argued convincingly that these cores must be truly prolate in order to satisfy the frequency and degree of elongation. Additionally, oblate cores with their plane coincidentally parallel to the filamentary cloud would be difficult to explain, especially since the velocity gradients parallel to the major axes are insufficient to account for rotational support, and hence flattening.

Observations of cores demonstrate a variety of sizes depending on the molecular line used (Myers et al. 1991a). Observations using a NH_3 line trace the densest regions, while CS, $C^{18}O$, ^{13}CO, and ^{12}CO all trace successively larger, and hence less dense, regions. One interesting result of this is that the less dense regions are more elongated, sometimes extending farther in only one direction (Fuller 1992). These density gradients along the elongated core's major axis correspond very well to the initial conditions used in Paper V to explore possible binary mass ratios.

Most cloud cores are found to be near virial equilibrium (Myers 1983; Loren 1989b). Considering the possible errors in determination of the cloud's density distribution and three-dimensional size, estimates of the cloud mass are probably uncertain by a factor of 2–4. A lower limit on J_0 for collapse to occur is ≈ 0.90 (Bastien 1983). From this we can gather that most clouds that form stars should have J_0 between 0.90 and ≈ 4. If these clouds are long-lived and close to stability, the distribution will be biased toward lower J_0 such that a typical value of J_0 of a star-forming cloud could be ≈ 1.5–2.0.

Cloud dynamics has also received much attention. Velocity gradients along filaments have been observed in Orion A (Bally et al. 1987) and Ophiuchus (Loren 1989b), among others. These velocity gradients, usually measured only in selected cuts parallel to the major axis, vary between 0.05 and 0.2 km s^{-1} pc^{-1} (Blitz 1991) and sometimes up to 0.5 km s^{-1} pc^{-1} (Loren 1989b). Velocity gradients in individual clumps can be significantly larger (0.2–5.9 km s^{-1} pc^{-1}; Loren 1989b). Velocity gradients in elongated cores have been investigated by Goodman et al. (1993; see also Fuller 1992). They found that the overall velocity gradient is typically ~ 1 km s^{-1} pc^{-1}. This corresponds to a value of β, the absolute value of the ratio of rotational to gravitational energies, of 0.02. Few clouds have β significantly larger than 0.04. Additionally, the direction of the velocity gradient has no obvious correlation with the direction of the major axis. Thus, rotation about an arbitrary axis with relatively small values of β are very good initial conditions for star formation (Paper IV).

3. MOLECULAR CORES: THE YSO ENVIRONMENT

Observations of molecular cores show a variety of morphologies, depending on whether or not they contain embedded YSOs. The morphologies and dynamics of molecular cores with embedded YSOs have been investigated extensively (see Rodríguez 1988 and references therein). Evidence of elongated structures around YSOs has usually been attributed to the presence of circumstellar disks and toroids (possibly rotationally supported). On the other hand, the elongated cores observed in filamentary molecular clouds have argued to be prolate by Myers et al. (1991a). The collapse calculations in Paper IV show that such prolate cores can lose their original morphology somewhat, as the denser matter surrounding the protostellar fragments is mostly rotationally supported and thus oblate. Thus an initially elongated prolate core forms a denser, smaller (by one order of magnitude or more), oblate, rotationally supported circumfragmentary envelope. These disks can be as large as ≈ 2000 AU (Paper IV) or as small as ≈ 100 AU (Paper V), depending on the value of J_0. The large-

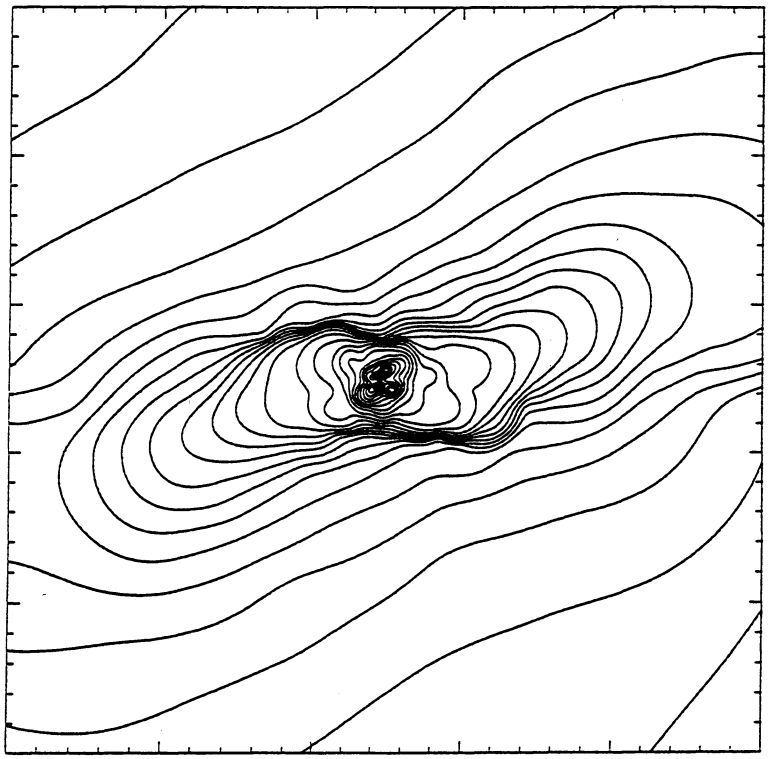

FIG. 1.—Contours of the column density for the simulation with $J_0 = 4$, $\beta_{\parallel} = 0.074$, and $\beta_{\perp} = 0.011$ from Paper IV. The step size between contours is 1.36.

scale disks compare well with the disks observed in polarization maps of YSOs (Bastien & Ménard 1990), while the small-scale disks compare with the scale assumed for actively accreting disks.

For calculations of the collapse of elongated clouds with rotation about an arbitrary axis, the component of the rotation parallel to the major axis results in the formation of the circumfragmentary disks/envelopes perpendicular to the cloud's major axis. The formation of two fragments with surrounding disks is a natural result of the fragmentation of elongated clouds with rotation about an arbitrary axis. The orbital motion of the fragment plus disk systems is roughly perpendicular to the plane of the disk. The exterior regions of the disk/envelope are therefore formed into a bow shape by gathering the slower moving cloud material. The higher density material is less affected because of its larger momentum. The two disks envelopes will interact at the center of the cloud, but the resulting oblate structure should still retain a signature of its past in the exterior regions. This is illustrated in Figure 1. The parameters used for computing the models used in this and other figures are given in Table 1. The exterior regions of the envelope are somewhat warped by their interaction with the surrounding medium, slowing them down so that they retain for longer periods an indication of the cloud core's original morphology. These exterior regions are not exactly disklike, in that they do not extend completely around the high-density region but are instead rather elongated, tracing the trajectories of the infalling gas. Observations of warped disks and/or envelopes around YSOs (see Rodríguez 1988) can therefore be taken as an indication of dynamical processes similar to fragmentation of elongated clouds. As the calculations often form binary or multiple systems, it should not be unexpected to have binary or multiple systems at the center of these warped disks, although it is not a necessary result.

For calculations with small amounts of rotation, and especially those without rotation parallel to the cloud's major axis, the two fragments form with a "bridge" of slightly lower density material connecting them. This material forms from the collapse of the cloud toward the major axis. The collapse in this direction is quicker than the collapse toward the equatorial plane even without rotation for elongations significantly greater than unity (Bonnell & Bastien 1991). In the case where two fragments form at equal distances from the equatorial plane, the matter in between feels little net force parallel to the major axis but only feels the combined force of both fragments (plus the rest of the cloud) toward the major axis. The relative importance of this "bridge" depends on the initial cloud structure. For an initially uniform cloud, the matter between the two fragments (see Fig. 2) is not as dense as it is for an initially centrally condensed cloud (Bonnell & Bastien 1993). The centrally condensed cloud has more matter between where the two

TABLE 1

SIMULATIONS INCLUDED IN THE FIGURES

Figure	J_0	$\beta_{\parallel}$	$\beta_{\perp}$	L/D	Reference
1	4.0	0.074	0.011	2.0	Paper IV
2	1.5	0.000	0.003	2.0	Paper V
3	1.8	0.000	0.010	2.0	Paper V
4	1.8	0.000	0.010	2.0	Paper V
5	2.0	0.000	0.020	2.0	Paper IV
6	2.0	0.041	0.020	2.0	Paper V
7	3.0	0.063	0.015	2.0	Paper IV
8	2.0	0.040	0.010	2.0	Paper IV

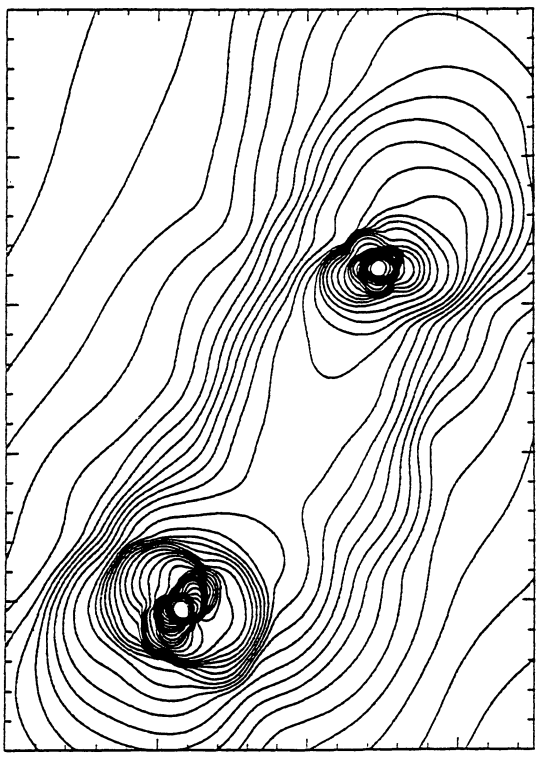

FIG. 2.—Contours of the column density for the simulation with $J_0 = 1.5$, $\beta_{\parallel} = 0.0$, and $\beta_{\perp} = 0.003$ from Paper V. The step size between contours is 1.41.

fragments form and therefore a better defined "bridge" of matter connecting them. This structure between the Binary Fragments has been observed in NGC 1333 IRAS 4 (Sandell et al. 1991), a very young binary system. Other examples of a connecting bridge of matter between the two components of a PMS binary are T Tau (Schwartz, Simon, & Campbell 1986), and DR 21(OH) (Padin et al. 1989).

4. KINEMATICS OF STAR-FORMING REGIONS

Studies of the kinematics of molecular clouds can be useful in determining the physical conditions in which stars form. Observed line widths have been extensively used as a measure of the cloud motions. Cloud cores with stars are found to have greater line widths than cores without stars (Benson & Myers 1989). Myers, Ladd, & Fuller (1991b) separated the cloud motions into thermal and nonthermal components. Their results indicate that the nonthermal motions increase more rapidly with the source luminosity than do the thermal components. Additionally, the nonthermal motions are at least partly due to the gas motions independent of the stars.

Loren (1989b) has investigated the kinematics in the filaments of Ophiuchus. In addition to finding the same distinction of higher line widths in cores with stars, he searched for velocity gradients along the filaments. Maps of the emission as a function of velocity and position along the filaments shows little evidence of a consistent velocity gradient. ΔV varies from 1 to 3 km s^{-1}, whereas rotation with an angular velocity of 3×10^{-14} s^{-1} produces a velocity difference of only 0.4 km s^{-1} pc^{-1}. However, velocity gradients have been observed in several other dense cores (e.g., Goodman et al. 1993).

The most prominent features in these velocity position plots for Ophiuchus are emission maxima that are extended in ΔV, relative to the surrounding cloud. At the same position, lower levels of emission have even greater ΔV. In fact, the largest values of ΔV are found at these locations.

These sudden increases in ΔV, indicating a local increase in the cloud's nonthermal motion, can be modeled as the result of dynamical processes. To see this, we consider the density at different line-of-sight velocities at positions along the cloud's major axis. In Figures 3 and 4 the column density as a function of velocity and position is shown for the collapse of an elongated cloud that forms a binary system. The two maxima at different positions with large spreads in velocity indicate the position of the two Binary Fragments. The appearance of the many small, unconnected high-density contours with a large spread in velocity, at the position of the lower fragment, is due to the dynamics of the fragments themselves. This would not be present if the density were convolved with a reasonable beam size. Additionally, emission from the high-density fragments could be obscured by a large optical depth.

In Figure 3 the cloud is viewed in a plane parallel to the rotation axis such that the rotational velocities are in the line of sight. The velocity gradient along the major axis is thus evident in Figure 3*a* and in the outer contours in Figures 3*b*, 3*c*, and 3*d*. The dynamic collapse of the cloud forms two fragments. The infall of material that forms and later on accretes onto each fragment produces the spread in velocities that are visible in Figures 3*b*, 3*c*, and 3*d*. In Figure 3*b* the second (upper) fragment is still forming; the maximum density at this position does not as yet show a large ΔV. At the density maximum, the slight change in velocity as a function of position indicates the local velocity gradient. This velocity gradient increases throughout the evolution at the position where the second (upper) fragment forms. The velocity gradient at the density maxima is in the same direction but is greater than the cloud's global velocity gradient.

The slight indications of the velocity gradient along the cloud's major axis are the slight difference of $V_{\rm LSR}$ at each end of the cloud and slight interdependence of the position and velocity for densities just below the maximum, indicative of a surrounding rotating disk. In contrast, Figure 4 shows the same evolution, except that the rotational velocities are no longer in the line of sight and are therefore not seen. The evolution is identical except for the aforementioned indications of rotation. The large values of ΔV at the positions of the two fragments are therefore independent of the cloud's rotation but are rather due to the dynamical infall of the cloud material onto the fragments.

The large ΔV associated with the dynamical infall onto a collapsing region can be used as an indication of where star formation is occurring before any protostellar object is formed. The extent to which dynamical collapse has occurred in particular regions can be judged by comparing with calculations such as those represented in Figures 3 and 4. Many such regions can be found in the position-velocity diagrams of the filaments in Ophiuchus, especially the L1689, L1712, L1729 filament (Loren 1989b).

Another way of investigating the kinematics of star-forming regions is by plotting the velocity of the emission peak against the position. Figure 5 shows the temporal evolution of the velocity gradient along a collapsing cloud's major axis. The velocity at each point is taken as the density-averaged velocity along the line of sight. This assumes that the gas is optically thin at the observed wavelength. The initially smooth velocity gradient is perturbed by the formation of the two fragments.

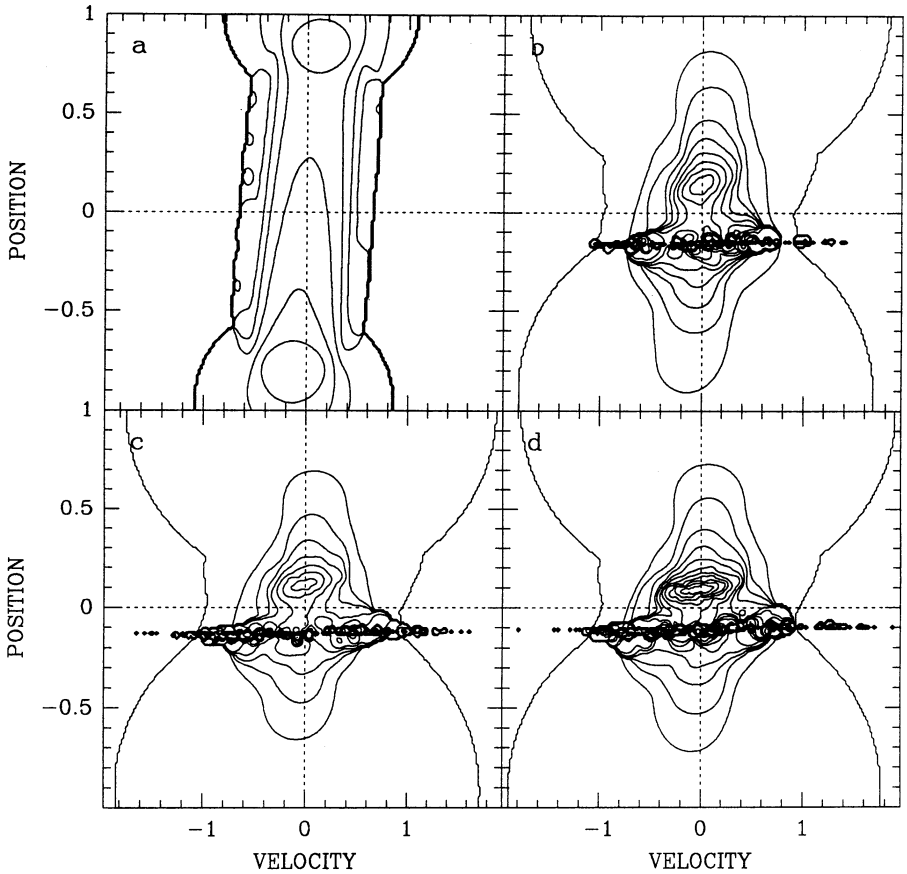

FIG. 3.—Contours of the column density as a function of position along the major axis and velocity in the line of sight. The rotational velocities are in the line of sight. The velocity scale is in km s^{-1}, and the position scale is in units where $L = 2$. The step sizes between contours are (*a*) 1.06, (*b*) 1.57, (*c*) 1.85, and (*d*) 1.59.

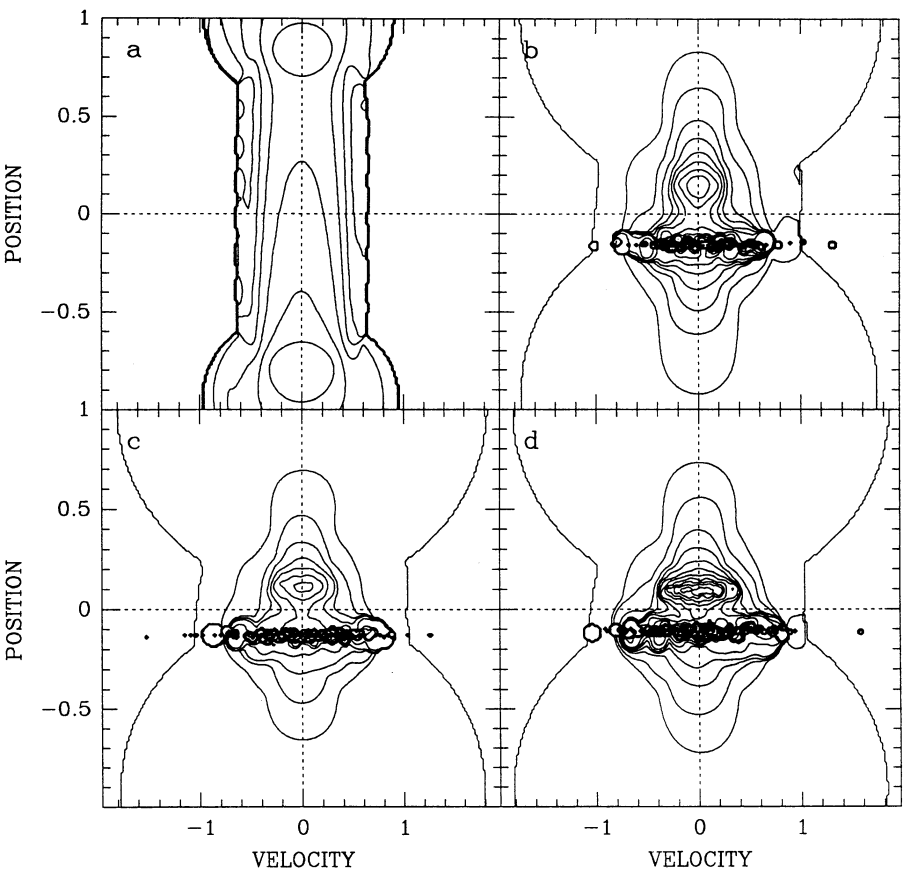

FIG. 4.—Same as Fig. 3, except that the rotational velocities are not in the line of sight. The step sizes between contours are (*a*) 1.06, (*b*) 1.55, (*c*) 1.85, and (*d*) 1.59.

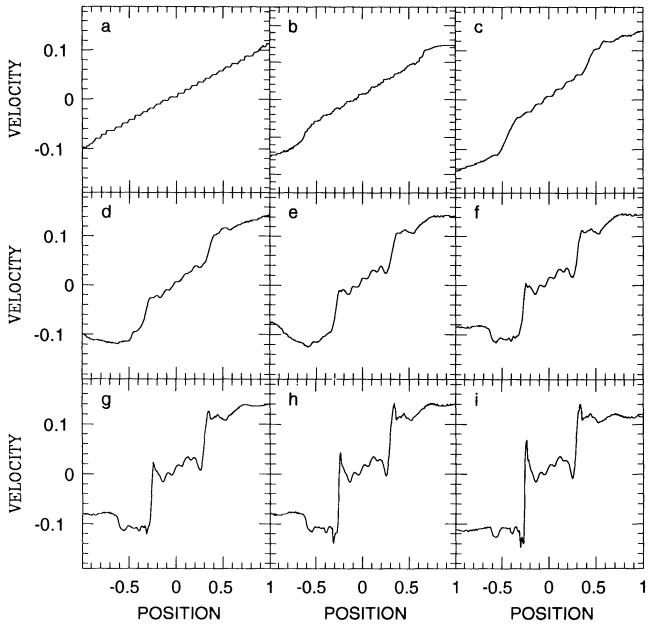

FIG. 5.—Density-averaged velocity gradients along the cloud's major axis for the simulation from $J_0 = 2$, $\beta_\perp = 0.02$, and $\beta_{||} = 0.0$. The temporal evolution is shown in panels *a–i*. The velocity scale is in km s^{-1}, and the position scale is in units where $L = 2$.

The velocity gradient increases at the location of each fragment, while keeping the same orientation as the overall velocity gradient. As the collapse proceeds and the two fragments increase in density, the velocity gradient increases dramatically until it is almost independent of position. The last panels show that the velocity gradient is very small exterior to the fragments and that the only significant change in velocity occurs at the fragments' locations.

A schematic of the expected velocity gradients for different objects is included in Figure 6. A rapidly rotating core has a velocity gradient that is steeper than the surrounding cloud owing to conservation of angular momentum (Fig. 6*a*). Once the core has collapsed and fragmented, the fragments have different velocities and the core's velocity gradient is approximately a step function with discontinuities at the fragments' positions (Fig. 6*b*). An outflow source will further complicate the core's velocity gradient (Fig. 6*c*; see Cabrit & Bertout 1990 for more details). It should be noted that observations with a realistic beam size could blur the distinction between the successive stages.

Large line widths in dense cores have often been understood as originating from an outflow. Myers et al. (1988) determined that the line widths in cores with outflows are significantly larger than those in cores without outflows. Wu, Zhou, & Evans (1992) point out that this may be misleading. The large line widths could be due to the process that forms the source of the outflows instead of the outflows themselves. Wu et al. (1992) separate their cores into three categories: (1) cores with sources and outflows, (2) cores with sources but without outflows, and (3) cores without sources or outflows. The line widths for each region are 0.87 ± 0.32 km s^{-1} for category 1, 0.71 ± 0.25 km s^{-1} for category 2, and 0.43 ± 0.13 km s^{-1} for category 3. This indicates that the majority of the difference between cores with and without outflows is that to have an outflow an exciting source is necessary. The formation of the source in a dense core generates larger line widths through the infall phase. Of course this does not imply that the outflows are not responsible for some of the large line widths observed. The cores with outflows in the Wu et al. (1992) data still have larger line widths than do the cores with stars, but without outflows. Additionally, large line widths may sometimes be due to dense gas seen in projection with the outflow as found in L43 (e.g., Mathieu et al. 1988).

5. COMPARISON WITH SELECTED STAR FORMATION REGIONS

5.1. *ρ Ophiuchi B1 and L1729*

The first region which we wish to compare with our numerical models of the fragmentation of elongated clouds and the formation of binary and multiple systems is ρ Ophiuchi B1. This region is part of a ridge of cores that extends from L1688 toward L1709 (Loren 1989a). B1 is part of the elongated core B and is also aligned with the elongated core C (Loren, Wootten, & Wilking 1990). The core B1 itself is oriented approximately perpendicular to the overall B-C ridge. Wadiak et al. (1985) and Sasselov & Rucinski (1990) have both found multiple clumps within the B1 core. Sasselov & Rucinski (1990) were able to resolve three clumps directly, while Wadiak et al. (1985) resolved two (possibly a third) clump by using the velocity structure. This velocity structure indicates rotation about an axis perpendicular to the line joining the two clumps. These two fragments probably have an aligned spin and orbital angular momenta. The third fragment, lying perpendicular to the line joining the two fragments, would therefore not be coplanar with them.

This system is very similar to one of the calculations reported in Paper V (see Fig. 8 in Paper V). Figure 7 shows a similar calculation, except with a slightly lower initial density gradient. In this calculation, the initial cloud has components of the rotation parallel and perpendicular to the cloud's major axis. Because of the rotation parallel to the major axis, the fragments

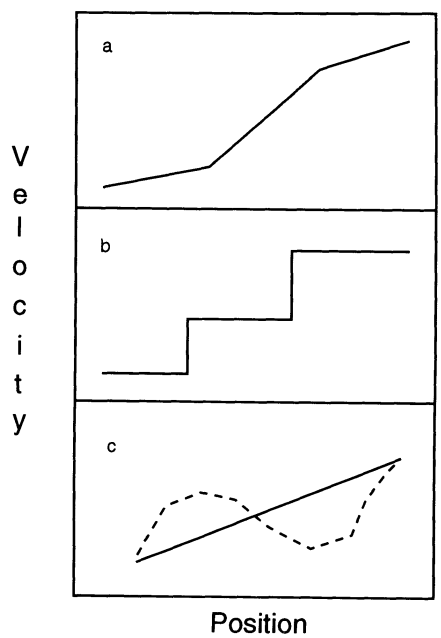

FIG. 6.—Schematic diagram of the expected velocity gradients from (*a*) a rapidly rotating core, (*b*) fragments at different velocities, and (*c*) a bipolar outflow.

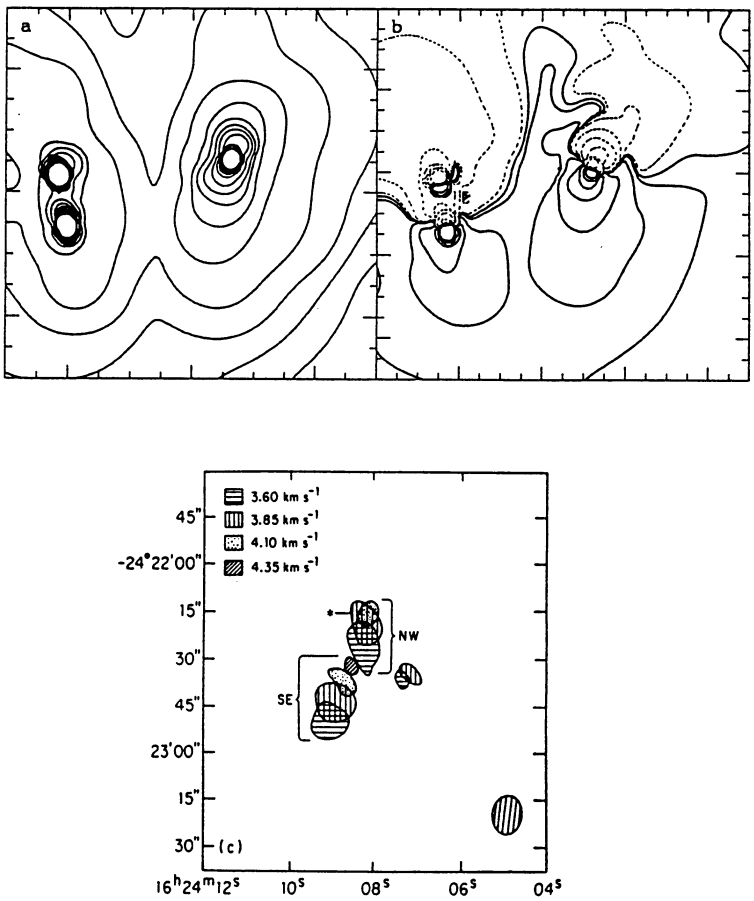

FIG. 7.—(*a*) Contours of the column density and (*b*) line-of-sight velocity structure for the simulation from $J_0 = 2$, $\beta_{\parallel} = 0.041$, and $\beta_{\perp} = 0.02$. The dotted and solid contours in (*b*) indicate negative and positive velocities, respectively. (*c*) Velocity structure of ρ Oph B1 taken from Wadiak et al. (1985).

form surrounded by disks, with rotational axes parallel to the cloud's major axis. There is an initial density gradient along the cloud allowing for unequal-mass fragments. The more massive fragment forms first with a relatively large disk, which fragments as a result of tidal forces with the other fragment and cloud. The resultant system is a noncoplanar triple system formed of a closer binary and a more distant and lower mass companion. The third companion's orbital plane is not parallel to that of the inner binary. The density and velocity structure of the system is shown in Figure 7. The velocity gradient in the inner binary is strongly reminiscent of that observed by Wadiak et al. (1985). All three components have approximately aligned spins. This is not always the case. Bonnell & Bastien (1992b) present a figure showing the density and velocity structure of a similar system where the third component's spin is not aligned with that of the other two.

The orientation of the B1 core, perpendicular to the overall B-C ridge (Loren et al. 1990), could then be explained as the oblate core resulting from the collapse of an elongated core parallel to the B-C ridge. The large velocity gradient across the fragments compared with the overall cloud (Wadiak et al. 1985) suggest that rotational support may not be negligible. An oblate, rotationally supported core is expected from the collapse of an elongated cloud with rotation parallel (and perpendicular) to the major axis.

Sasselov & Rucinski (1990) find that the three clumps in the B1 core have mass, size, density, and temperature that fit well into the isothermal collapse stage. Furthermore, the velocity-position diagram of the region (Loren 1989b), passing nearby but not directly through the B1 core, has lower level emission extended in velocity that could indicate dynamical infall (see above).

Another region of interest in Ophiuchus is L1729. In Loren's (1989a) designation, R75 contains two maxima which appear elongated perpendicular to the overall core and filament. In the context of the fragmentation of elongated clouds with rotation about an arbitrary axis (Paper IV), the two maxima would be the rotationally supported oblate envelope out of which the fragments form. Figure 8 illustrates such a calculation. Furthermore, the velocity-position diagrams of L1729 (Loren 1989b) show that at least one of the maxima is extended in its velocity range, which may indicate infall (see above).

5.2. *NGC 2024*

NGC 2024 is a site of recent star formation within the Orion B cloud. It is one of a series of star-forming regions that fall along the major axis of Orion B (Maddalena et al. 1986). Lada et al. (1991) have surveyed the general region and found 42 dense CS cores, the cores associated with NGC 2024 being among the most prominent ones. These cores have significant elongations with an average projected aspect ratio of 1.8. A 2.2 μm survey of the same region has found many near-infrared sources, including 309 sources associated with NGC 2024 (Lada 1990). The elongated core in NGC 2024 is also aligned

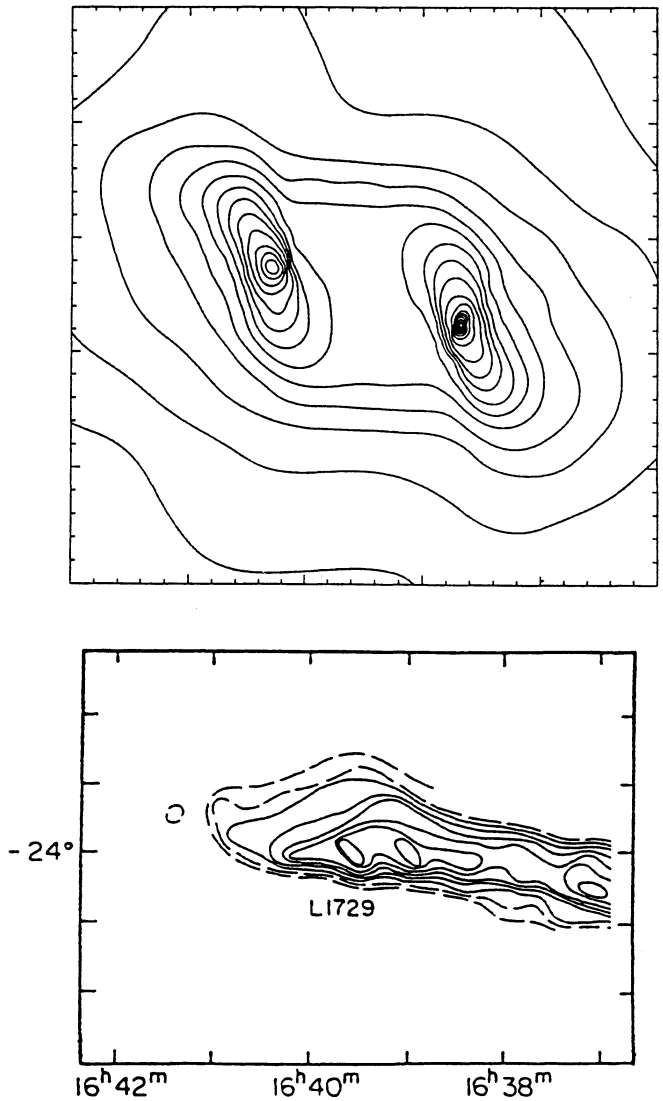

FIG. 8.—Two disk-like structures approximately perpendicular to the cloud's major axis from numerical simulations (*top*) and Lynds 1729 (*bottom*) (Loren 1989a) with a beam size of 2'.4 (the ticks correspond to 10'). The direction of the cloud elongation in the top panel is horizontal, as indicated by the lower level contours. The step size between contours is 1.55.

with the surrounding elongated dust lane (Schulz et al. 1991). The alignment of the elongated structure over different scales seems to imply that the region is truly prolate.

Mezger et al. (1988) reported the detection of six far-infrared objects embedded within the elongated NGC 2024 core. These embedded sources are aligned with the cloud's major axis. Mezger et al. (1988) argue that the six objects are true isothermal protostars (i.e., they lack an internal energy source), while Moore et al. (1989) deduce that significant heating has occurred and that the objects are heavily obscured luminous stellar cores (i.e., heating due to contraction of an optically thick object or to ongoing nuclear burning). A systematic velocity gradient parallel to the core's major axis is observed (Lis, Carlstrom, & Phillips 1991; Schulz et al. 1991). Significant increases in ΔV are also present at the positions of several of the far-infrared sources (Lis et al. 1991; Schulz et al. 1991), as would be expected from an infall phase (see § 4 above). A position-velocity diagram of NGC 2024 showing the velocity gradient and the extended ΔV's is included in Figure 9 (taken from Schulz et al. 1991). Barnes & Crutcher (1990) have found evidence for a rotating semicircular structure which they interpret as being either an expanding torus or a small cluster of fragments on eccentric orbits. The fragmentary nature of the semicircular structure would tend, at least at first approach, to support the hypothesis of a few condensations formed through the fragmentation of a disklike structure.

The combination of an elongated, probably prolate, structure with a velocity gradient along its major axis and several aligned condensations embedded in the NGC 2024 dense core is highly reminiscent of the calculations presented in Papers III, IV, and V. The presence of increased ΔV at the position of the far-infrared sources combined with the possibility of the subfragmentation of one of the condensations makes the comparison almost complete.

5.3. *Lynds 1551 IRS 5*

Lynds 1551 IRS 5 is one of the most studied of YSOs. It is a deeply embedded source that is believed to be the source of a molecular outflow and optical jet (Lada 1985; Stocke et al. 1988). Lynds 1551 also contains the YSO sources XZ Tau (binary; see Haas, Leinert, & Zinnecker 1990). HL Tau L1551NE, L1551W, and the source VLA 1. The region is further complicated by the presence of many jets and outflows (Mundt, Ray, & Bührke 1988; Pound & Bally 1991).

Molecular observations of the circumstellar structure of L1551 IRS 5 have shown an elongated structure approximately perpendicular to the bipolar outflow (Kaifu et al. 1984; Sargent et al. 1988). CS observations show a large-scale (2×10^4 AU) structure at position angle P.A. = 160° (Kaifu et al. 1984). Kaifu et al. (1984) also reported a large-scale velocity gradient, but it has not been confirmed by subsequent observations (Batrla & Menton 1985; Menton & Walmsley 1985). CO observations show a medium-scale (3600 AU) elongated structure with P.A. = 160° and a smaller scale (1500 AU) structure with P.A. = 135° (Sargent et al. 1988). The medium-scale CO observations also show some evidence for a velocity gradient along the major axis, but it is unclear whether it can be

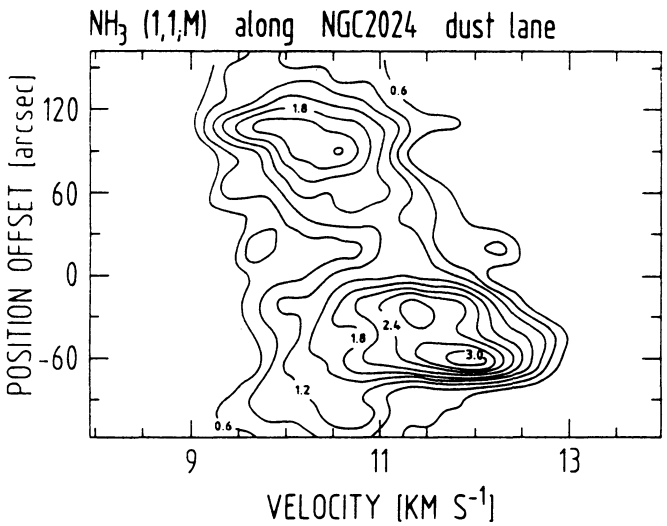

FIG. 9.—Position-velocity diagram along the major axis of NGC 2024, taken from Schulz et al. (1991).

attributed to Keplerian rotation (see also Goodman et al. 1993). Near-infrared polarization measurements also indicate extended structure with P.A. = 160° (Nagata, Sato, & Kobayashi 1983). The difference in position angle at different scales is in agreement with what is expected from the collapse of an elongated cloud rotating about an arbitrary axis (see Fig. 1 and § 3 above). Furthermore, the lack of a sufficient velocity gradient to indicate rotation is appropriate, since the extended regions at different position angles are not rotationally supported but instead are remnant infall, slowed down by interacting with the cloud medium (see § 3 above and Paper IV).

Radio observations with much greater resolution have detected two sources separated by 50 AU (Bieging & Cohen 1985; Rodríguez et al. 1986). The position angle of the line between these two sources is again different, P.A. = 190° Bieging & Cohen (1985) interpret the two sources as being a binary system, while Rodríguez et al. (1986) interpret them as being the inner, ionized walls of a circumstellar toroid. The toroid would presumably help collimate the flow, except that the position angle is off by 30°. Rodríguez et al. (1986) reject the idea of a binary system because of the extended emission around the two sources. This emission is extended perpendicular to the line connecting the two sources and is centered in between them, thus possibly on the undetected exciting star.

Figure 10 shows the column density contours of the central part of a collapsing elongated cloud core rotating about an arbitrary axis similar to that shown in Figure 1. Fragmentation into two parts due to the cloud's initial shape, followed by subfragmentation, has formed a multiple system. The surrounding cloud matter is elongated in the direction perpendicular to the cloud's major axis and is truly oblate owing to rotational support. This structure is the remains of the two circumfragmentary disks that have collided at the cloud's center. The morphology of this matter is very similar to that mapped by Rodríguez et al. (1986) around the two radio sources. Furthermore, even the detailed structure in the radio map is reproduced in Figure 10.

One additional observation that may shed some light on the complexities of L1551 IRS 5 is the possibility of a second bipolar outflow that may originate from L1551 IRS 5 (Moriarty-Schieven & Wannier 1991). The presence of a second outflow would be difficult to explain from a single source.

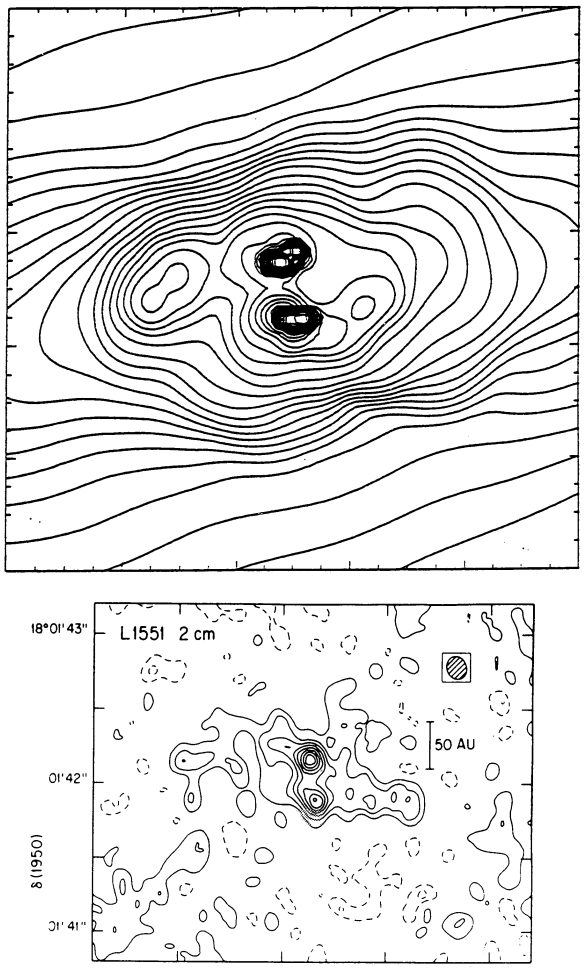

FIG. 10.—(*Top*) Column density contours around a hierarchical quadruple system. The structure around the system is suggestive of the 2 cm VLA map of Lynds 1551 IRS 5 (*bottom*) (taken from Rodríguez et al. 1986). The step size between contours in the top panel is 1.30.

6. PRE–MAIN-SEQUENCE BINARIES

Systematic searches for PMS binaries have only recently been undertaken. Using a variety of techniques including spectroscopy (Mathieu, Walter, & Myers 1989), speckle interferometry (Zinnecker et al. 1991; Ghez, Neugebauer, & Matthews 1992; Leinert et al. 1992), lunar occultation (Simon et al. 1987; Chen et al. 1990; Simon et al. 1992; Leinert et al. 1991), and near-infrared imaging (Zinnecker 1988; Moneti & Zinnecker 1991; Zinnecker, Brandner, & Reipurth 1992), the numbers of PMS binaries for all orbital periods have increased up to and possibly beyond the main-sequence frequencies. The surveys suggest that most, if not all, T Tauri stars are members of binaries. There also seems to be no difference in the binary frequency of classical and weak-lined T Tauri stars (Leinert et al. 1992; Ghez et al. 1992; Simon 1992), indicating that active accretion disks can exist in the binary environment.

Orbital eccentricities of the spectroscopic PMS binaries have a dependency on the orbital period similar to that in main-sequence stars (Mathieu 1992); i.e., the distribution has a maximum eccentricity increasing with the period (Duquennoy & Major 1991). The only difference is that the maximum period at which all orbits are circular is 4 days, compared with the 11 day maximum for main-sequence stars (Mathieu 1992). The difference is thought to represent the distances to which tidal circularization has had time to operate. Since the PMS binary frequency and orbital parameters are comparable to those on the main sequence, whatever mechanism is responsible for the formation of binary stars has already occurred by the PMS stage. Reviews of PMS binaries can be found in Reipurth (1988), Zinnecker (1989), and Bodenheimer, Ruzmaikina, & Mathieu (1992).

6.1. *Reddening and IR Companions*

The formation of binary stars through a fragmentation or other noncapture scenario implies that the two components are approximately coeval. This offers the possibility of comparing the PMS evolution of different-mass stars.

Infrared observations of pre–main-sequence binaries have ascertained that frequently the more luminous component is redder (Zinnecker 1989; Moneti & Zinnecker 1991). It is difficult to apply a mass-luminosity relation to PMS stars which may have their luminosities affected by accretion from and scattering by a disk. It is nevertheless possible that the more

luminous IR companion is the more massive object. This is of course the opposite of the main-sequence relation, where the less massive component is redder. Furthermore, a number of IR companions, not detectable in the visible, have been observed in systems with an optically visible T Tauri star (e.g., DoAr24E, Glass I [Chelli et al. 1988]; T Tau [Ghez et al. 1991]; Haro 6-19 [Leinert & Haas 1989]; Z CMa [Koresko et al. 1991; Haas et al. 1992]; and XZ Tau [Haas et al. 1990]). In some cases (Glass I, Haro 6-10, Z CMa, and T Tau) the IR companion is more luminous and thus possibly more massive. Evaluating their evolutionary stage by their spectral energy distribution would seem to dispute that the two components are approximately the same age. The optically visible component is a T Tau star (class II or class III; see Adams, Lada, & Shu 1987) while the IR companion is a class I object. For a review on IR companions see Zinnecker & Wilking (1992).

The solution to these discrepancies is to be found in the differences in accretion processes in binary versus single stars. Single stars accrete through a spherically symmetric infall stage (class I object), followed by accretion through a circumstellar disk (class II object). The circumstellar disk is formed by infalling matter with nonzero angular momentum. This matter cannot be accreted directly and must undergo a process where angular momentum is removed to allow for accretion.

Although the same general processes occur in a binary system, the dynamics are complicated by the binary's orbital motion. The spherically symmetric infall is directed toward the system's center of mass. In an unequal mass binary, the primary is always closer to the center of mass and will therefore preferentially receive this matter. The matter with appreciable angular momentum such that it forms into a disk will have a tendency to orbit the cloud's center of mass which can be approximated as the position of the primary. The secondary, also orbiting the same point, will have comparable rotation to the adjacent matter and will thus be able to accrete it without the necessity of removing the excess angular momentum through a disk process. The secondary therefore has a smaller tendency to be obscured by the spherically symmetric infall or to be surrounded by a circumstellar disk than does the primary. The infall onto an unequal-mass binary is illustrated in Figure 11. Additionally, the gravitational torques which will increase accretion at closest approach will have a greater effect on the secondary's disk than on the primary's (Zinnecker 1989; Paper V), owing to the difference in fragment masses. Thus, any disk possessed by the secondary is likely to be quickly decimated by the tidal forces at closest approach. Thus, the secondary will evolve faster from the class I stage and will have a much smaller and shorter-lived disk, enabling it to pass more quickly through the class II stage.

Another observational effect of a reddened or infrared companion would be a modification of the spectral energy distribution (SED). The SED has been used to classify the evolutionary status of YSOs (Adams et al.; Lada 1991). The flat SEDs of some T Tauri stars have been hard to explain in the conventional sense of a young star plus disk. Adams, Lada, & Shu (1988) tried to model these objects using an unorthodox temperature distribution which is difficult to envision in either an active or a passive accretion disk (Bertout 1989). If, instead of trying to model the source with a simple star plus disk, we add an infrared companion with a class I SED, the normally decreasing SED longward of 2.2 μm will be offset by the class I's rising SED. The result can then be a flat SED. One of the sources that Adams et al. (1988) modeled was the flat SED of T Tau. In arguing against the possibility that the SED is affected by the IR companion, they neglected the effects of the companion's disk and infall. Ghez et al. (1991) were able to separate the SED of T Tau into two components. The optical component (T Tau N) is then a class II object with a decreasing slope, while the IR companion (T Tau S) dominates the IR excess. The combination of the two SEDs gives the overall flat SED. Zinnecker & Wilking (1992) estimate that about 10% of PMS binaries have IR companions. They also suggest that these systems are significantly younger than the average PMS star. A scenario where PMS binaries evolve through a stage where one star is an IR companion could help explain the flat SEDs.

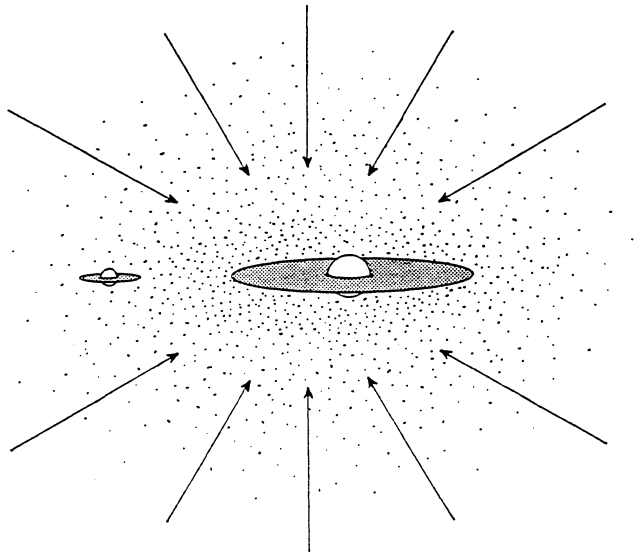

FIG. 11.—Schematic of the infall onto an unequal-mass binary. The spherically symmetric infall is toward the center of mass, which is close to the primary. The secondary is located away from the center of mass and accretes mainly from the matter gathered in the primary's disk.

7. MAIN-SEQUENCE BINARIES

The frequency of stellar duplicity has been investigated repeatedly (i.e., Abt & Levy 1976, hereafter AL; Duquennoy & Mayor 1991, hereafter DM). AL stated that there are 1.4 companions per primary with a binary frequency of 67%, which can increase close to 100% considering undetected lower mass companions. More recent studies (DM) put the binary frequency of G dwarfs at about 57% in the solar neighborhood. Incorporating possible incompleteness and undetected low-mass secondaries, up to 67% of stars are in binaries or multiple systems. It is therefore important for any model of star formation to include relatively large probabilities of forming binary and multiple systems. For a comparison of different theoretical models with observations the reader is referred to Zinnecker (1984) and Boss (1988). The fragmentation of elongated clouds is able to form binary systems for $J_0 \geq 1.5$ (Papers IV and V), with relatively low values of β. Compared with the collapse of spherically symmetric clouds with initial density perturbations, elongated clouds closer to gravitational equilibrium and with less rotational energy can form binary systems more easily.

7.1. *Separation and Eccentricity*

The dynamical properties of binary systems can be characterized by three parameters: the orbital separation, the orbit's eccentricity, and the sysem's mass ratio. Separations of main-

sequence binary stars range from a few solar radii to 0.1 pc. The frequency-period relation can be fitted by a Gaussian with a maximum at 180 yr (DM) corresponding to about 100 AU. The distribution of orbital eccentricities can be separated into three parts depending on the binary period (DM). For periods up to about 10 days, the eccentricity is zero because of tidal circularization. For periods between 10 and 1000 days, the eccentricity distribution is bell-shaped with a mean of $e = 0.3$. At greater periods, the eccentricity distribution increases with increasing eccentricity according to $f(e) = 2e$. In general, this implies that few if any binary systems should form with completely circular orbits.

The binary systems formed through the fragmentation of elongated clouds have a high initial eccentricity (0.4–0.9; Paper III; Paper IV; Paper V). The actual value depends on the parameters J_0, L/D, and $\beta_\perp$. In simpler, slightly idealized terms, the orbit is determined by the fragments' masses, the cloud's angular momentum about an axis perpendicular to the cloud's major axis, and the separation at which the two fragments form. Assuming that a fixed amount of the cloud's angular momentum is deposited in the two fragments, the separation at periastron is proportional to the square of the cloud's angular momentum and inversely proportional to the cube of the fragments' masses. The separation at apastron is determined by the distance at which the two Binary Fragments form, with some modification due to dissipative effects of the cloud medium. Therefore, for a given fragment mass and initial separation, increasing the cloud's angular momentum will decrease the eccentricity. Alternatively, for a given fragment mass and cloud angular momentum, an increase in the initial separation will increase both the eccentricity and the period. The observed increase in maximum eccentricity with increasing period (DM) can then be explained by the increase in initial separation of the two components at the time of formation. This difference in initial separations is easily explained by the different lengths and elongations of the initial cloud.

Once the upper limit of the eccentricity-period relation is established, it is necessary to be able to explain the spread in eccentricities lower than this maximum at each period. The eccentricity can be reduced in three ways from its maximum value by increasing the cloud's angular momentum perpendicular to the cloud's major axis (i.e., $\beta_\perp$), by disk-disk dissipative interactions, and by accretion. The first is very easy to envision: by increasing the cloud's angular momentum, you increase the separation at periastron. A limitation of this is that clouds tend to have relatively small values of β (Fuller 1992; Goodman et al. 1993).

Disk-disk dissipative encounters hold more promise. Calculations with a nonzero $\beta_\parallel$ form binaries with disks that are parallel but not collinear (Paper IV). These disks do not lie in the orbital plane, and thus at periastron a component of the orbital motion is perpendicular to the plane of the disk. Direct disk-disk interactions can then dissipate some of the orbital velocity and thus reduce the eccentricity. Paper IV gives a few examples of this mechanism where the eccentricity is decreased from 0.79 ($\beta_\parallel = 0.000$) to 0.55 ($\beta_\parallel = 0.010$) and from 0.70 ($\beta_\parallel = 0.000$) to 0.43 ($\beta_\parallel = 0.010$) and 0.30 ($\beta_\parallel = 0.016$). Another effect of these disk-disk interactions is that they will also reduce the separation at apastron and therefore the orbital period. This scenario is similar to that proposed by Clarke & Pringle (1991), except that the decomposition of the rotation into two components reduces the direct dependency between the separation at periastron and the eccentricity.

Additionally, continued accretion in an eccentric binary can also reduce the eccentricity (Paper V). The infalling matter that is not directly incorporated into one of the two fragments forms a disk in the same plane as the binary's orbit. Each fragment continues to accrete from this reservoir. The orbit is modified by the relative angular momentum of the accreted matter. This matter is in a more or less circular orbit, at least compared with the binary, around the cloud's center of mass. The accretion can reduce or increase the fragment's orbital angular momentum, depending on when it takes place. At periastron, matter with lower orbital angular momentum is accreted, and this reduces the fragment's orbital angular momentum. At apastron, the accreted matter in a circular orbit has greater orbital angular momentum, increasing the fragment's orbital angular momentum. The decrease of orbital angular momentum at periastron reduces the apastron distance, while increasing the orbital angular momentum at apastron increases the periastron distance. The continued accretion therefore tends to reduce the system's eccentricity.

The periastron separations of the binary systems formed in Papers III, IV, and V range from $\simeq 50$ to 4000 AU. These values will increase slightly with the decrease in eccentricity. It should also be noted that apastron separations are on average 5 times greater. Separations greater than 4000 AU are not difficult to produce in this model; they only require larger initial cloud dimensions. The fragment masses need not increase proportionately if the cloud has a greater elongation. Systems with smaller separations could also be formed by reducing the initial cloud dimensions, but this would also reduce the fragment's mass. Alternatively, smaller separations could be produced by a smaller value of $\beta_\perp$. This would form a binary system with smaller periastron distance but larger eccentricity. Eccentricity damping by disk-disk interactions would then be important. Closer systems are more likely to dissipate greater amounts of angular momentum through this process, as the smaller separation would increase the disk-disk interaction. This would also explain the decreasing eccentricity with decreasing separation (DM). Resolution limits in the simulations are presently not adequate to explore such close systems, because of the isothermal approximation in the equation of state.

7.2. *Mass Ratios*

The frequency distribution of binary mass ratios—defined as $q = m_2/m_1$, where m_1 and m_2 are the masses of the primary and secondary, respectively—has been determined by several authors (see, for example, Tout 1991; DM). A bimodal distribution was observed by Trimble (1974) and AL. AL also determined that the peak at 1.0 was represented by close systems, while that for unequal-mass systems was represented by more distant systems. They argue that two different formation modes produce the equal- and unequal-mass secondaries, respectively, the equal-mass systems by a fragmentation process and the unequal mass systems either by fission or by capture. Supporting this assessment, the bimodal distribution, with peaks at 1.0 and 0.3, corresponds to the unimodal distributions of the double-lined (SB2) and single-lined (SB1) spectroscopic binaries, respectively (Staniucha 1979).

Unfortunately, selection effects have played an important role in the determination of the mass-ratio distribution (e.g., Trimble 1990; DM). Taking into account the overabundance of SB2's due to selection effects, the peak at $q = 1.0$ is strongly downplayed and may be absent. Other studies taking selection

effects into account have also found distributions that do not have a peak at $q = 1$ (Halbwachs 1987). Instead, they find a smoothly rising distribution with decreasing q with a maximum around $q = 0.3$. Additionally, Halbwachs (1987) determined that there is no difference between the distribution of mass ratios for short- and long-period binaries. Thus all binaries could be formed by the same process. Tout (1991) has investigated the possibility that the binary mass-ratio distribution arises from the pairing of stars with masses chosen randomly according to the initial mass function. He has found that simple selection effects can account for the observed distributions of SB1's and SB2's.

DM's observations of binary systems of solar-type stars in the solar neighborhood offer the most complete sample, which should avoid selection effects. Their determinations of the distribution of mass ratios show no peak at $q = 1$ but rather increasing frequency with decreasing q until a maximum is reached at $q = 0.23$. The distribution is either flat or decreasing for lower values of q. Additionally, no dependence of the mass-ratio distribution on the orbital separation was found.

Comparing the observed binary mass-ratio distribution with theoretical models involves the various fragmentation modes discussed in Paper IV. The most common mode, Binary Fragmentation, involving the structural fragmentation of elongated clouds, has been investigated in terms of possible mass ratios in Paper V. Mass ratios of binary systems formed through other modes (Disk Fragmentation, Bar Fragmentation, Bar-Arm Fragmentation), can be found in Papers IV and V.

Binary Fragmentation in an elongated cloud with an initial density gradient parallel to its major axis can form binary systems with mass ratios from 0.065 to 1.0 (Paper V). The masses of the fragments are defined by the central regions which are not supported by rotation or by thermal energy and would therefore continue to collapse if a minimum smoothing length were not present (see Paper IV). No statistical investigation of the density gradients present in elongated molecular cloud cores has been undertaken, so it is presently impossible to predict a distribution quantitatively. What is certain is that these asymmetries do exist and that only small density gradients are required to cover the whole range of observed mass ratios in binary stars (Paper V).

Perfect symmetry is, of course, unexpected in an object as large and diffuse as a molecular cloud core. A qualitative estimate of the distribution of asymmetries in cores could therefore be a Gaussian with a maximum at a small nonzero asymmetry, corresponding to a density gradient of a few percent. This would ensure that the distribution of mass ratios would decrease toward mass ratios of unity.

Possibilities of a lower limit or decreasing frequency for mass ratios less than 0.2 (i.e., DM) arise from the tidal dissipation of one fragment by its companion (Paper IV). Systems that form with greatly unequal mass components will form the more massive component first and the less massive one later. Because of their movement toward each other while they are forming, if the secondary has a much smaller mass than does the primary, it will form much closer to the primary and thus will undergo a larger tidal force. If this tidal force is large enough, it can completely dissipate the secondary, removing binary systems with low mass ratios from the distribution. Although the distances involved (e.g., $\sim$100–1000 AU) are much greater than those commonly cited for tidal effects to be important, it is the ratio of the object's size to the perturber's distance which is important. The formation of a protostellar object involves the condensation of a large and relatively diffuse body of gas, such that tidal forces can be important over large distances.

Boss (1981) investigated the collapse and fragmentation of a rotating spherical cloud in the presence of a tidal perturbation. He found that for a large tidal perturbation, no collapse occurs; instead, material piled up at the edge of the boundary nearest the perturber. In a simulation where no boundary separates the two objects, the matter which is impeded from collapsing by the tidal forces will instead be accreted by the perturber (Paper IV). The ratio of tidal to gravitational energies, δ, necessary to prevent the collapse is $\delta > 4$. For an uniform-density sphere of mass M and radius R, perturbed by a punctual source of mass m^* located at a distance r^* away from the center of the sphere, δ is given by (Boss 1981)

$$\delta = \frac{5}{12}\left(\frac{m^*}{M}\right)\left(\frac{2R}{r^*}\right).$$

For a perturber that is placed at approximately the sphere's radius $r^* = R$, the condition $\delta > 4$ reduces to

$$m^* > 4.8M .$$

This implies that tidal dissipation of the secondary by the primary can be important for systems with mass ratios $q \leq 0.21$. This limit assumes that the secondary forms very close to the primary. This assumption is plausible in the case of the collapse and fragmentation of elongated clouds with relatively low J_0 (i.e., $J_0 \approx 1.5$) but is less valid for clouds with high J_0. Clouds with higher J_0 would have lower limits to the mass ratio, but the probability of clouds with large J_0 decreases with increasing J_0 if most clouds are close to equilibrium. From this we can conclude that the distribution of mass ratios reported by DM can plausibly be reproduced by the fragmentation of elongated clouds via a Binary Fragmentation mechanism (Papers III, IV, and V).

Other modes of fragmentation discussed in Paper IV are Bar Fragmentation, Bar-Arm Fragmentation, and Disk Fragmentation. These modes occur in the subfragmentation of one of the condensations formed through a Binary Fragmentation. Although all of these modes occurred in the context of forming multiple systems in Paper IV, it was demonstrated in Paper V that these modes could occur, forming a simple binary, without any distant companions. In these cases, the second Binary Fragment failed to coalesce because of the initial density gradient along the cloud's major axis. The mass ratios cited for these fragmentation modes varies between 0.2 and 1.0.

Bar Fragmentation formed equal mass fragments but in the presence of tidal forces would be transformed into Bar-Arm Fragmentation, where the two subcondensations have a typical mass ratio of 0.8. Disk Fragmentation, the fragmentation of one of the circumfragmentary disks due to tidal forces, can form a wide variety of mass ratios, ranging between 0.15 and 0.87 (Papers IV and V). A possible lower limit to the mass ratio formed by Disk Fragmentation can be found in the stability analysis of circumstellar disks (Adams, Ruden, & Shu 1989; Shu et al. 1990). Shu et al. (1990) found that a maximum mass can be calculated for which the disk would be stable against an $m = 1$ perturbation. This value is approximately 0.32 times the mass of the central object. Assuming that the stability analysis of disks to $m = 1$ perturbations (Shu et al. 1990) is somewhat appropriate for the tidally induced Disk Fragmentation reported in Papers IV and V, it is important to

note that incomplete incorporation of the disk matter into the newly formed fragment will reduce the expected mass ratio. Nevertheless, a plausible decrease in the frequency of forming binary systems with $q < 0.2$ (i.e., due to disk stability against fragmentation) can be envisioned.

Overall, the distribution of mass ratios from the combined processes of Disk Fragmentation, Bar Fragmentation, and Bar-Arm Fragmentation can be gathered from the probability of occurrence. Bar and Bar-Arm Fragmentation require slightly larger values of $\beta_{\|}$ and J_0 than does Disk Fragmentation. Observational estimates of rotation and gravitational stability in molecular clouds (i.e., Goodman et al. 1993) predict that the cloud cores are close to virial equilibrium. This implies that there is an increasing frequency of clouds with decreasing values of β and J_0, with peak values of $\beta \approx 0.02$ and $J_0 \approx 2$. An implication of this is that Disk Fragmentation is more likely to occur than Bar or Bar-Arm Fragmentation. Taking into account the different mass ratios expected for each process, an increasing frequency with decreasing q is plausible. As mentioned above, the decrease at low q can also be explained by stability arguments of circumstellar disks.

8. MULTIPLE STARS

Although direct measurements of stellar multiplicity have determined the ratio of doubles to triples to quadruples to be 46:9:2 (AL) and 40:7:2 (DM), indirect studies suggest that up to 50% of binaries are in triple or quadruple systems (Mayor & Mazeh 1987; Mazeh 1990). The frequency of multiple systems that include eclipsing binaries has also been studied by Chambliss (1992). The frequency of multiple systems in Papers III, IV, and V is dependent on the probability of initial conditions where $J_0 \geq 2$ and significant rotation ($\beta_{\|} \geq 0.015$) is present.

Observational properties of multiple systems offer an additional opportunity of comparison with theoretical models. Multiple systems can retain more information about their prenatal cloud dynamics than do binary systems. Fekel (1981) investigated the possibility of orbital coplanarity among multiple systems. In his sample, coplanarity is not possible for 35% of the multiple systems. Coplanarity is not certain but remains a possibility for the other systems. This lower limit on the frequency of noncoplanar multiple systems implies that processes that form only coplanar multiple systems (i.e., Bodenheimer 1978; Norman & Wilson 1978; Boss 1991; Paper III) cannot account for all of the observed multiple systems. Alternatively, the fragmentation of elongated clouds with rotation about an arbitrary axis (Paper IV; Paper V) can form multiple systems where the orbital plane of an inner binary has no relation to the orbital plane of the outer system. In these cases, a binary or coplanar multiple system forms on one side of the elongated cloud, while a single, binary, or coplanar multiple system forms on the other side. The orbital plane of each inner system is defined by the perpendicular to the axis of rotation. The orbital planes of the inner systems are therefore parallel. If the initial rotation is not purely "end over end," i.e., rotation around an axis perpendicular to the cloud's major axis, then the line joining the two systems formed on either side of the cloud is not parallel to either system's orbital plane. The two orbital planes are therefore parallel but not coplanar. Furthermore, the orbital motion of each system, around the cloud's center of mass, occurs in a plane defined by the cloud's major axis and the perpendicular to the component of the rotation perpendicular to that axis.

Fekel (1981) also investigated the mass ratios of his sample of multiple systems. Although selection effects are possible (see Tout 1991), the observed triple systems show that the mass ratio of the more distant companion and the closer binary is usually smaller than that of the binary. Furthermore, there is a greater range in mass ratios of the outer than of the inner system. If this is not due to a selection effect (most of the inner systems are SB2's), then this could indicate a different formation process. In comparison, the fragmentation of elongated clouds forms two major components which can have a wide range of mass ratios (Paper V), with no apparent lower limit. Each major component can subfragment directly (Bar Fragmentation; see Paper IV), or through its circumfragmentary disk (Disk Fragmentation; see Paper IV). Although mass ratios for these processes range from 0.2 to 1.0, a lower limit on the mass ratio is possible because of disk stability requirements (Shu et al. 1990). In the few evolutions where mass ratios were calculated for triple systems in Paper V, the mass ratio for the outer combined system has a lower average (0.27) than that of the inner binary (0.52). Only one inner binary had a lower mass ratio than the outer system.

9. SUMMARY AND CONCLUSIONS

1. Observations of molecular cloud cores indicate initial conditions for the onset of gravitational collapse and star formation. The observed properties include elongated prolate structures with projected aspect ratios of ≈ 2–4, rotation about arbitrary axes with low values of β (Goodman et al. 1993), and asymmetries in the cloud which can be represented as slight density gradients along the core's major axis. These initial conditions have been used in Papers I–V as the initial conditions for the formation of binary and multiple systems.

2. The environment of YSOs has been observed to consist of elongated, disklike structures. The circumfragmentary disks formed in Papers III, IV, and V have sizes ranging from that of an actively accreting disk to the large-scale disks observed in polarization studies (Bastien & Ménard 1990). In some observations the position angle of the disklike structure is found to depend on the distance from the central source. These structures have been interpreted as rotationally supported disks even when the evidence for rotational support is weak. The simulations reported in Paper IV form such objects which are only partially rotationally supported and have position angles which vary with distance because of interactions with the cloud medium.

The formation of a binary system from an elongated core often involves the formation of a "bridge" of matter connecting the two fragments. Such structures have been observed to connect PMS binaries.

3. The kinematics of molecular clouds can give clues as to the ongoing processes. The gravitational collapse and infall of a molecular cloud increase the line width at the location of the forming condensation. An increase in the line width can therefore be an indication of the location of gravitational collapse and infall. In a rotating cloud, the local velocity gradient in the forming condensation is larger than that of the total cloud.

4. Several star formation regions display structures and dynamics that are similar to those formed through the collapse and fragmentation of elongated clouds. The presence of an elongated core containing a noncoplanar multiple system with a surrounding oblate envelope combined with large line widths indicative of infall all occur in ρ Ophiuchi B1. These features are all to be found in the results of Papers IV and V. Other

regions in which similarities to the structures formed in Papers III, IV, and V are found include Lynds 1729 and Lynds 1551 IRS 5. The inner double radio sources observed in Lynds 1551 IRS 5 by Bieging & Cohen (1985) and Rodríguez et al. (1986) could be related to a binary system, even though they lie perpendicular to the structure of the gas between them.

5. The differential reddening in PMS binaries and the existence of IR companions find a natural explanation in the formation and continuing accretion of unequal-mass binary systems (see Paper V). The more massive primary accretes either spherically symmetrically or through a surrounding disk. The less massive secondary, in contrast, receives less of the spherically symmetric infall, owing to its location away from the system's center of mass. Instead, the secondary can accrete the matter accumulated in the disk around the primary, especially at closest approach. No transfer of angular momentum is necessary, since the secondary's orbital velocity is similar to that of the matter in the primary's disk. The secondary is thus likely to have considerably less surrounding matter, which means less reddening.

6. The observed properties of main-sequence solar-type stars include large eccentricities for periods greater than that for tidal circularization (DM). The binary systems formed in Papers III, IV, and V can have arbitrarily large eccentricities (<1), while systems with lower eccentricities can be formed by disk-disk dissipative encounters at closest approach (Paper IV). The binary systems formed in Papers III, IV, and V have separations greater than or equal to 50 AU. Forming binaries with smaller separations requires greater resolution but is plausible within the proposed models.

7. The observed distribution of mass ratios (DM) can also be reproduced with the results from Papers IV and V with plausible assumptions about the initial conditions. Small initial asymmetries result in the formation of unequal-mass binaries such that prolate clouds would have to be almost perfectly symmetrical with respect to their equatorial plane in order to form exactly equal-mass systems. A decreasing frequency of occurrence is therefore expected with mass ratios approaching unity. A possible decrease in the frequency of systems with mass ratios less than ≈ 0.2 might be expected as a result of the effects of tidal forces on the formation of the secondary. Systems that attempt to form with mass ratios $\lesssim 0.2$ will undergo tidal effects which could completely dissipate the secondary if they form close enough together.

Similar distributions of the mass ratio can also be expected from the Bar and Disk Fragmentation process. In these cases, arguments about the frequency of clouds with larger J_0 and β imply a difference in the frequency of each process, while a lower mass ratio cutoff could arise from the disk stability requirements (Shu et al. 1990).

8. Observations of multiple systems show that at least 35% of them are noncoplanar (Fekel 1981). The multiple systems formed through the fragmentation of elongated clouds with rotation about an arbitrary axis can form such noncoplanar systems. Furthermore, the observed difference in mass ratios between the outer and inner systems can be explained by the different processes involved in the formation of a multiple system.

We would like to thank Hans Zinnecker, Phil Myers, and Peter Barnes for stimulating discussions, and Giselle Glackmeyer for preparing Figure 11. We also thank the referee, Alyssa Goodman, for comments which significantly improved the paper and suggesting Figure 6. The authors are grateful to the Conseil de Recherche en Sciences Naturelles et en Génie (CRSNG) du Canada for financial assistance. This research would not have been possible without the CNI (Calcul Numérique Intensif) facilities of the Université de Montréal.

REFERENCES

Abt, H. A., & Levy, S. G. 1976, ApJS, 30, 273 (AL)
Adams, F., Lada, C. J., & Shu, F. H. 1987, ApJ, 312, 788
———. 1988, ApJ, 326, 865
Adams, F., Ruden, S., & Shu, F. 1989, ApJ, 347, 959
Arcoragi, J.-P. Bonnell, I., Martel, H., Benz, W., & Bastien, P. 1991, ApJ, 380, 476 (Paper II)
Bally, J., Langer, W. D., Stark, A. A., & Wilson, R. W. 1987, ApJ, 312, L45
Barnes, P. J., & Crutcher, R. M. 1990, ApJ, 351, 176
Bastien, P. 1983, A&A, 119, 109
Bastien, P., Arcoragi, J.-P., Benz, W., Bonnell, I., & Martel, H. 1991, ApJ, 378, 255 (Paper I)
Bastien, P., & Ménard, F. 1990, ApJ, 364, 232
Batrla, W., & Menton, K. M. 1985, ApJ, 298, L19
Benson, P. J., & Myers, P. C. 1989, ApJS, 71, 89
Bertout, C. 1989, ARA&A, 27, 351
Bieging, J. H., & Cohen, M. 1985, ApJ, 289, L5
Blitz, L. 1991, in The Physics of Star Formation and Early Stellar Evolution, ed. C. J. Lada & N. D. Kylafis (Dordrecht: Kluwer), 3
Bodenheimer, P. 1978, ApJ, 224, 488
Bodenheimer, P., Ruzmaikina, T., & Mathieu, R. D. 1992, in Protostars and Planets III, ed. E. H. Levy & J. Lunine (Tucson: Univ. Arizona Press), in press
Bonnell, I., Arcoragi, J.-P., Martel, H., & Bastien, P. 1992, ApJ, 400, 579 (Paper IV)
Bonnell, I., & Bastien, P. 1991, ApJ, 374, 610
———. 1992a, ApJ, 401, 654 (Paper V)
———. 1992b, in IAU Colloq. 135, Complementary Approaches to Double and Multiple Star Research, ed. W. Hartkopf & H. McAlister (San Francisco: ASP), in press
———. 1993, in preparation
Bonnell, I., Martel, H., Bastien, P., Arcoragi, J.-P., & Benz, W. 1991, ApJ, 377, 553 (Paper III)
Boss, A. P. 1981, ApJ, 246, 866
———. 1988, Comm. Astrophysics, 12, 169
———. 1991, Nature, 351, 298
Cabrit, S., & Bertout, C. 1990, ApJ, 348, 530
Chambliss, C. R. 1992, PASP, 104, 663
Chelli, A., Zinnecker, H., Carrasco, L., Cruz-Gonzalez, I., & Perrier, C. 1988, A&A, 207, 46
Chen, W. P., Simon, M., Longmore, A. J., Howell, R. R., & Benson, J. A. 1990, ApJ, 357, 224
Clarke, C., & Pringle, J. 1991, MNRAS, 249, 588
Duquennoy, A., & Mayor, M. 1991, A&A, 248, 485 (DM)
Dutrey, A., Langer, W. D., Bally, J., Duvert, G., & Wilson, R. W. 1991, A&A, 247, L9
Fekel, F. C. 1981, ApJ, 246, 879
Fuller, G. A. 1992, in Workshop on Galactic Star Formation, ed. J. P. Arcoragi, P. Bastien, & R. E. Pudritz (Montreal: Univ. Montreal), in press
Ghez, A. M., Neugebauer, G., Gorham, P., Haniff, C. A., Kulkarni, S. R., Matthews, K., Koresko, C., & Beckwith, S. 1991, AJ, 102, 2066
Ghez, A. M., Neugebauer, G., & Matthews, K. 1992, in IAU Colloq. 135, Complementary Approaches to Double and Multiple Star Research, ed. W. Hartkopf & H. McAlister (San Francisco: ASP), in press
Goodman, A. A., Benson, P. J., Fuller, G. A., & Myers, P. C. 1993, ApJ, in press
Haas, M., Christou, J., Zinnecker, H., Ridgway, S. T., & Leinert, C. 1992, A&A, in press
Haas, M., Leinert, C., & Zinnecker, H. 1990, A&A, 230, L1
Halbwachs, J. L. 1987, A&A, 183, 234
Kaifu, N., et al. 1984, A&A, 134, 7
Koresko, C. D., Beckwith, S. V. W., Ghez, A. M., Matthews, K., & Neugebauer, G. 1991, AJ, 102, 2073
Lada, C. 1985, ARA&A, 23, 267
———. 1991, in The Physics of Star Formation and Early Stellar Evolution, ed. C. J. Lada & N. D. Kylafis (Dordrecht: Kluwer), 329
Lada, E. 1990, in Physical Process in Fragmentation and Star Formation, ed. R. Capuzzo-Dolcetta, C. Chiosi, & A. Di Fazio (Dordrecht: Kluwer), 193
Lada, E., Bally, J., & Stark, A. 1991, ApJ, 368, 432
Larson, R. B. 1972, MNRAS, 156, 437
Leinert, Ch., & Haas, M. 1989, ApJ, 342, L39
Leinert, Ch., Haas, M., Richichi, A., Zinnecker, H., & Mundt, R. 1991, A&A, 250, 407
Leinert, Ch., et al. 1992, IAU Colloq. 135, Complementary Approaches to Double and Multiple Star Research, ed. W. Hartkopf & H. McAlister (San Francisco: ASP), in press

Lis, D. C., Carlstrom, J. E., & Phillips, T. G. 1991, ApJ, 370, 583
Loren, R. B. 1989a, ApJ, 338, 902
———. 1989b, ApJ, 338, 925
Loren, R. B., Wootten, A., & Wilking, B. A. 1990, ApJ, 365, 269
Maddalena, R. J., Morris, M., Moscowitz, J., & Thaddeus, P. 1986, ApJ, 303, 375
Mathieu, R. D. 1992, in The Realm of the Interacting Binary Stars, ed. J. Sahade, G. McCluskey, & Y. Kondo (Dordrecht: Kluwer), in press
Mathieu, R. D., Benson, P. J., Fuller, G. A., Myers, P. C., & Schild, R. E. 1988, ApJ, 330, 385
Mathieu, R. D., Walter, F. M., & Myers, P. C. 1989, AJ, 98, 987
Mayor, M., & Mazeh, T. 1987, A&A, 171, 157
Mazeh, T. 1990, AJ, 99, 675
Menton, K. M., & Walmsley, C. M. 1985, A&A, 146, 369
Mezger, P. G., Chini, R., Kreysa, E., Wink, J. E., & Salter, C. J. 1988, A&A, 191, 44
Moneti, A., & Zinnecker, H. 1991, A&A, 242, 428
Moore, T. J. T., Chandler, C. J., Gear, W. K., & Mountain, C. M. 1989, MNRAS, 237, 1P
Moriarty-Schieven, G. H., & Wannier, P. G. 1991, ApJ, 373, L23
Mundt, R., Ray, T. P., & Bührke, T. 1988, ApJ, 333, L69
Myers, P. C. 1983, ApJ, 270, 105
Myers, P. C., Fuller, G., Goodman, A. A., & Benson, J. 1991a, ApJ, 376, 561
Myers, P. C., Heyer, M., Snell, R. L., & Goldsmith, P. F. 1988, ApJ, 324, 907
Myers, P. C., Ladd, E., & Fuller, G. 1991b, ApJ, 372, L95
Nagata, T., Sato, S., & Kobayashi, Y. 1983, A&A, 119, L1
Norman, M., & Wilson, J. 1978, ApJ, 224, 497
Padin, S., et al. 1989, ApJ, 337, L45
Pound, M. W., & Bally, J. 1991, ApJ, 383, 705
Reipurth, B. 1988, in Formation and Evolution of Low Mass Stars, ed. A. K. Dupree & M. T. V. T. Lago (Dordrecht: Kluwer), 305
Rodríguez, L. F. 1988, in Galactic and Extragalactic Star Formation, ed. R. E. Pudritz & M. Fich (Dordrecht: Kluwer), 97
Rodríguez, L. F., Cantó, J., Torrelles, J. M., & Ho, P. T. P. 1986, ApJ, 301, L25
Rouleau, F., & Bastien, P. 1990, ApJ, 355, 172
Sandell, G., Aspin, C., Duncan, W., Russell, A. P. G., & Robson, E. I. 1991, ApJ, 376, L17
Sargent, A. I., Beckwith, S., Keene, J., & Masson, C. 1988, ApJ, 333, 936
Sasselov, D. D., & Rucinski, S. M. 1990, ApJ, 351, 578
Schneider, S., & Elmegreen, B. G. 1979, ApJS, 41, 87
Schulz, A., Gusten, R., Zylka, R., & Serabyn, E. 1991, A&A, 246, 570
Schwartz, P. R., Simon, T., & Campbell, R. 1986, ApJ, 303, 233
Shu, F., Tremaine, S., Adams, F., & Ruden, S. 1990, ApJ, 358, 495
Simon, M. 1992, in IAU Colloq. 135, Complementary Approaches to Double and Multiple Star Research, ed. W. Hartkopf & H. McAlister (San Francisco: ASP), in press
Simon, M., Howell, R. R., Longmore, A. J., Wilking, B. A., Peterson, D. M., & Chen, W. P. 1987, ApJ, 320, 344
Simon, M., Chen, W. P., Howell, R. R., Benson, J. A., & Slowik, D. 1992, ApJ, 384, 212
Staniucha, M. 1979, Acta Astron., 29, 587
Stocke, J. T., Hartigan, P., Strom, S. E., Strom, K. M., Anderson, E. R., Hartmann, L. W., & Kenyon, S. J. 1988, ApJS, 68, 229
Tout, C. A. 1991, MNRAS, 250, 701
Trimble, V. 1974, AJ, 79, 967
———. 1990, MNRAS, 242, 79
Ungerechts, H., & Thaddeus, P. 1987, ApJS, 63, 645
Wadiak, E. J., Wilson, T. L., Rood, R. T., & Johnston, K. L. 1985, ApJ, 295, L43
Wu, Y., Zhou, S., & Evans, N. J. 1992, ApJ, 394, 196
Zinnecker, H. 1984, Ap&SS, 99, 41
———. 1988, in Formation and Evolution of Low Mass Stars, ed. A. K. Dupree & M. T. V. T. Lago (Dordrecht: Kluwer), 111
———. 1989, in Low-Mass Star Formation and Pre–Main Sequence Objects, ed. B. Reipurth (Munich: ESO), 447
Zinnecker, H., Brandner, W., & Reipurth, B. 1992, in IAU Colloq. 135, Complementary Approaches to Double and Multiple Star Research, ed. W. Hartkopf & H. McAlister (San Francisco: ASP), in press
Zinnecker, H., Christou, J. C. Ridgway, S. T., & Probst, R. G. 1991. in Astrophysics with Infrared Arrays, ed. R. Elston (San Francisco: ASP), 271
Zinnecker, H., & Wilking, B. A. 1992, in Binary Stars as Tracers of Stellar Formation, ed. A. Duquennoy & M. Mayor (Cambridge: Cambridge Univ. Press), in press